Anomalous photon-assisted tunneling in graphene

2012 J. Phys.: Condens. Matter 24 015303

(http://iopscience.iop.org/0953-8984/24/1/015303)

Report Documentation Page

Form Approved
OMB No. 0704-0188

1. REPORT DATE	2. REPORT TYPE	3. DATES COVERED
18 DEC 2011		**00-00-2011 to 00-00-2011**

4. TITLE AND SUBTITLE	5a. CONTRACT NUMBER
Anomalous Photon-Assisted Tunneling In Graphene	5b. GRANT NUMBER
	5c. PROGRAM ELEMENT NUMBER
6. AUTHOR(S)	5d. PROJECT NUMBER
	5e. TASK NUMBER
	5f. WORK UNIT NUMBER
7. PERFORMING ORGANIZATION NAME(S) AND ADDRESS(ES) **Air Force Research Laboratory (ARFL/RVSS),Kirtland Air Force Base,NM,87117**	8. PERFORMING ORGANIZATION REPORT NUMBER
9. SPONSORING/MONITORING AGENCY NAME(S) AND ADDRESS(ES)	10. SPONSOR/MONITOR'S ACRONYM(S)
	11. SPONSOR/MONITOR'S REPORT NUMBER(S)

12. DISTRIBUTION/AVAILABILITY STATEMENT
Approved for public release; distribution unlimited

13. SUPPLEMENTARY NOTES
Journal Of Physics: Condensed Matter, (2012)(8pp)

14. ABSTRACT

15. SUBJECT TERMS

16. SECURITY CLASSIFICATION OF:			17. LIMITATION OF ABSTRACT	18. NUMBER OF PAGES	19a. NAME OF RESPONSIBLE PERSON
a. REPORT	b. ABSTRACT	c. THIS PAGE			
unclassified	**unclassified**	**unclassified**	**Same as Report (SAR)**	**10**	

J. Phys.: Condens. Matter **24** (2012) 015303 (8pp) doi:10.1088/0953-8984/24/1/015303

Anomalous photon-assisted tunneling in graphene

Andrii Iurov[1], Godfrey Gumbs[1,2], Oleksiy Roslyak[1] and Danhong Huang[3]

[1] Department of Physics and Astronomy, Hunter College, City University of New York, 695 Park Avenue, New York, NY 10065, USA
[2] Donostia International Physics Center (DIPC), P de Manuel Lardizabal, 4, 20018 San Sebastian, Basque Country, Spain
[3] Air Force Research Laboratory (ARFL/RVSS), Kirtland Air Force Base, NM 87117, USA

Received 6 August 2011, in final form 21 October 2011
Published 8 December 2011
Online at stacks.iop.org/JPhysCM/24/015303

Abstract
We investigated the transmission of Dirac electrons through a potential barrier in the presence of circularly polarized light. An anomalous photon-assisted enhanced transmission is predicted and explained. It is demonstrated that the perfect transmission for nearly head-on collision in infinite graphene is suppressed in gapped dressed states of electrons, which is further accompanied by a shift of peaks as a function of the incident angle away from head-on collision. In addition, the perfect transmission is partially suppressed by a photon-induced gap in illuminated graphene. After the effect of rough edges of the potential barrier or impurity scattering is included, the perfect transmission with no potential barrier becomes completely suppressed and the energy range for the photon-assisted transmission is reduced at the same time.

(Some figures may appear in colour only in the online journal)

1. Introduction

Research activity on the properties of graphene has been growing rapidly ever since its experimental discovery and the demonstration of its unusual properties arising from its energy band structure [1, 2]. The novel properties of graphene may be attributed to its massless Dirac fermions at the Fermi energy [3]. An interesting consequence of the Dirac electron is the Klein paradox [4], in which an electron in graphene undergoes unimpeded tunneling through potential barriers of arbitrary height and thickness. This property of the Dirac electrons is due to their linear energy dispersion relation or helicity. Electrons are said to be chiral if their wavefunctions are eigenstates of the chirality operator $\hat{h} = \boldsymbol{\sigma} \cdot \mathbf{p}/(2p)$, where $\boldsymbol{\sigma} = \{\sigma_x, \sigma_y\}$ is the Pauli vector consisting of Pauli matrices and $\mathbf{p} = \{p_x, p_y\}$ is the electron momentum in he graphene layers. Electrons in graphene near the K points (around the corners of the hexagonal Brillouin zone) are chiral due to the fact that the chirality operator is proportional to the Dirac Hamiltonian which automatically makes chirality a good quantum number.

The fact that the Klein paradox is also obtained in bilayer graphene makes this effect even more sophisticated. This leads us to realize that the Klein paradox is not simply due to linear electron dispersion but may be observed for both massless and massive quasiparticles [4]. In this paper, we consider a sharp p–n–p junction or potential barrier profile. This type of potential can be constructed by an underlying metal contact or an insulating strip [5] and has been employed to demonstrate unimpeded transmission [3]. Apart from using an optical field, one may also create potential barriers (p–n junctions) as well as energy gaps and coherence using the surface curvature as discussed in the paper by Atanasov and Saxena [6].

Both the tight-binding model and the $\mathbf{k}\cdot\mathbf{p}$ approximations for an infinite graphene sheet accurately show that electrons and holes have linear energy dispersions $\varepsilon(k) = s\hbar v_{\mathrm{F}}k = s\hbar v_{\mathrm{F}}\sqrt{k_x^2 + k_y^2}$ with no gap, where s is the electron–hole parity with $s = 1$ for electrons and $s = -1$ for holes. For the potential barrier described above, there is a translational symmetry in the y direction parallel to the boundaries of the potential so that k_y is conserved. In contrast, the longitudinal component k_x is modified by the potential so that when the particle has energy E we have $k_{x,i} = (\hbar v_{\mathrm{F}})^{-1}\sqrt{(E - V_0)^2 - (\hbar v_{\mathrm{F}}k_y)^2}$, where V_i is the potential in the region i.

The electron effective mass and its properties will play a crucial role in our analysis. In infinite intrinsic graphene, the Dirac electron is massless although the mass can be introduced [7] or implemented experimentally. For bilayer graphene, the particle effective mass exists in any possible

approximation [8], leading to the existence of evanescent terms in the wavefunction [4], although this does not violate chirality symmetry and the Klein paradox.

The outline of the rest of this paper is as follows. In section 2, we derive the eigenstates and transmission coefficient for Dirac electrons dressed with photons from a circularly polarized light. Section 3 is devoted to a formalism in which the roughness of the boundaries for the potential barrier is included phenomenologically in calculating the transmission coefficient; numerical results are also presented. A brief summary is given in section 4.

2. Transmission coefficient for dressed electron states

It was shown recently [9, 10] that when Dirac electrons in a single graphene layer are interacting with an intense circularly polarized light, the electron states will be dressed by photons. The main idea of the present study is to investigate the transmission properties of such dressed electrons for the case of single layer graphene. We go beyond the approximations used in [9] by retaining the results up to the order of $\mathcal{O}(\Delta^4)$ so that we are able to investigate the difference between the dressed states and the massive Dirac electrons described below by the Hamiltonian in (24). Here, Δ is a quantity measuring the induced gap between the valence and conduction bands of the dressed electrons.

We begin with the electron–photon interaction Hamiltonian

$$\mathcal{H} = v_{\mathrm{F}}\sigma \cdot (\mathbf{p} - e\,\mathbf{A}_{\mathrm{circ}}), \tag{1}$$

where v_{F} is the Fermi velocity and the vector potential for circularly polarized light of frequency ω_0 can be expressed as

$$\mathbf{A}_{\mathrm{circ}} = \sqrt{\frac{\hbar}{\epsilon_0\,\omega_0 V}}(\mathbf{e}_+\hat{a} + \mathbf{e}_-\hat{a}^\dagger)$$
$$= \sqrt{\frac{\hbar}{2\epsilon_0\,\omega_0 V}}[(\hat{a} + \hat{a}^\dagger)\mathbf{e}_x + \mathrm{i}(\hat{a} - \hat{a}^\dagger)\mathbf{e}_y] \tag{2}$$

in terms of photon creation and destruction operators $\hat{a}^\dagger$ and $\hat{a}^\dagger$, respectively. Here, V is the mode volume of an optical field. In order to study the complete electron–photon interacting system, we must add the field energy term $\hbar\omega_0\,\hat{a}^\dagger\hat{a}$ to the Hamiltonian (1). As usual, we seek the wavefunction in the form of a plane wave $\Psi(\mathbf{r}) = \mathrm{e}^{\mathbf{i}\mathbf{k}\cdot\mathbf{r}}\psi(k)$, which results in the following reduced Hamiltonian:

$$\mathcal{H} = \hbar\omega_0\,\hat{a}^\dagger\hat{a} + \hbar v_{\mathrm{F}}\sigma\cdot\mathbf{k} - \sqrt{\frac{2\hbar e^2 v_{\mathrm{F}}^2}{\epsilon_0\,\omega_0 V}}(\sigma_+\hat{a} + \sigma_-\hat{a}^\dagger), \tag{3}$$

where $\sigma_+ = \frac{1}{2}(\sigma_x + \mathrm{i}\sigma_y) = \left[\begin{smallmatrix}0 & 1\\ 0 & 0\end{smallmatrix}\right]$ and $\sigma_- = \frac{1}{2}(\sigma_x - \mathrm{i}\sigma_y) = \left[\begin{smallmatrix}0 & 0\\ 1 & 0\end{smallmatrix}\right]$. The reduced Hamiltonian (3) for infinite graphene can be understood as the sum of two parts, namely, the Dirac Hamiltonian

$$\mathcal{H}_{\mathrm{Dirac}} = \hbar v_{\mathrm{F}}\,\sigma\cdot\mathbf{k} = \hbar v_{\mathrm{F}}(\sigma_x k_x + \sigma_y k_y)$$
$$= \hbar v_{\mathrm{F}}(\sigma_- k_+ + \sigma_+ k_-) \tag{4}$$

and the Jaynes–Cummings Hamiltonian

$$\mathcal{H}_{\mathrm{J-C}} = \hbar\omega_0\,\hat{a}^\dagger\hat{a} - \frac{w}{2\sqrt{N}}(\sigma_+\hat{a} + \sigma_-\hat{a}^\dagger), \tag{5}$$

which corresponds to a two-level quantum optical system and, most importantly, can be solved analytically. Here, we have defined $k_\pm = k_x \pm \mathrm{i}k_y$ and N represents the number of radiation quanta (intensity) for the incident optical field. We only consider the situation such that the electron–photon interaction amplitude w is much less than either the photon or the Dirac electron energy, i.e.,

$$w = 2\sqrt{\frac{2N\hbar e^2 v_{\mathrm{F}}^2}{\epsilon_0\,\omega_0 V}} = 2\alpha\,\hbar\omega_0 \ll \hbar\omega_0, \tag{6}$$

where $\alpha \equiv w/\hbar\omega_0 \ll 1$. The two eigenstates of the Hamiltonian (5) could be obtained with an expansion over the basis of just two functions $|1\rangle_N \equiv |\uparrow, N\rangle$ and $|2\rangle_N \equiv |\downarrow, N{+}1\rangle$ for each N value, that is,

$$|\Psi_{\uparrow,N}\rangle = \mu_N|1\rangle_N + \nu_N|2\rangle_N, \tag{7}$$

$$|\Psi_{\downarrow,N}\rangle = \mu_N|2\rangle_N - \nu_N|1\rangle_N, \tag{8}$$

which corresponds to the following Hamiltonian in the chosen basis $|1\rangle_N$ and $|2\rangle_N$:

$$\mathcal{H}_N = \begin{bmatrix} h_{11} & h_{12}\\ h_{21} & h_{22}\end{bmatrix} = \hbar\omega_0\begin{bmatrix} N & \mp\frac{\alpha}{2}\sqrt{\frac{N+1}{N}}\\ \mp\frac{\alpha}{2}\sqrt{\frac{N+1}{N}} & N+1\end{bmatrix}. \tag{9}$$

In this way, the transformation (7) and (8) becomes just a simple rotation in the Hilbert space. This expansion yields the eigenvalue equation and its solution below:

$$(\varepsilon - N\hbar\omega_0)[\varepsilon - (N+1)\hbar\omega_0] - \left(\frac{\alpha}{2}\,\hbar\omega_0\sqrt{\frac{N+1}{N}}\right)^2 = 0, \tag{10}$$

$$\varepsilon_{\uparrow\downarrow} = \left(N + \frac{1}{2}\right)\hbar\omega_0 \mp \frac{\hbar\omega_0}{2}\sqrt{1 + \alpha^2\left(\frac{N+1}{N}\right)}$$
$$\backsimeq \left(N + \frac{1}{2} \mp \frac{1}{2}\right)\hbar\omega_0 \mp \frac{\alpha^2}{4}\hbar\omega_0, \tag{11}$$

where $\epsilon_\uparrow$ and $\epsilon_\downarrow$ correspond to the lower $+$ and upper $-$ signs in the solution. For simplicity, we assume here that the radiation is classically strong with $N \gg 1$. However, we note that we may set $N + 1 \backsimeq N$ only in the terms $\mathcal{O}(\alpha^2)$ but not in the terms with $N\hbar\omega_0$. Furthermore, it is a simple matter to obtain the expansion coefficients μ_N and ν_N as

$$\mu_N = \cos\theta_c \backsimeq 1 - \frac{\alpha^2}{8},$$
$$\nu_N = \sin\theta_c \backsimeq \frac{\alpha}{2}, \tag{12}$$
$$\tan\theta_c = \frac{\alpha\sqrt{(N+1)/N}}{1 + \sqrt{1 + \alpha^2(N+1)/N}} \backsimeq \frac{\alpha}{2}.$$

One can easily verify that the wavefunctions (7) and (8) are the eigenstates of the Jaynes–Cummings Hamiltonian (5) with

energies (11), to any order of α. Here, for all the above derivations, we have employed the standard relations, i.e.,

$$\begin{aligned} \hat{a}^{\dagger}|\uparrow\downarrow, N\rangle &= \sqrt{N+1}|\uparrow\downarrow, N+1\rangle, \\ \hat{a}|\uparrow\downarrow, N\rangle &= \sqrt{N}|\uparrow\downarrow, N-1\rangle, \\ \sigma_{+}|\downarrow, N\rangle &= |\uparrow, N\rangle, \qquad \sigma_{+}|\uparrow, N\rangle = 0, \\ \sigma_{-}|\uparrow, N\rangle &= |\downarrow, N\rangle, \qquad \sigma_{-}|\downarrow, N\rangle = 0. \end{aligned} \tag{13}$$

We now look for the eigenstates of the Hamiltonian (3) as expansions over the set of Jaynes–Cummings Hamiltonian eigenfunctions (7) and (8). We will confine our attention to the field source with only three nearest photon occupation numbers, i.e., $N = N_0 - 1$, N_0 and $N_0 + 1$, leading to

$$|\Phi(k)\rangle \backsim \sum_{\ell=N_0-1}^{N_0+1} \left(\mathcal{C}_{1,\ell}(k)|\Psi_{\uparrow,\ell}\rangle + \mathcal{C}_{2,\ell}(k)|\Psi_{\downarrow,\ell}\rangle\right). \tag{14}$$

We know that the eigenfunctions (7), (8) corresponding to different numbers N are orthogonal to each other. First acting the Hamiltonian (3) on (14), and then multiplying both sides of the expansion (14) by $\langle\Psi_{\uparrow,N_0}|$, $\langle\Psi_{\downarrow,N_0-1}|$, $\langle\Psi_{\uparrow,N_0+1}|$ and $\langle\Psi_{\downarrow,N_0}|$, this results in the following four equations:

$$\begin{aligned} &\mathcal{C}_{1,N_0}\left(N_0 - \frac{\alpha^2}{4}\frac{N_0+1}{N_0}\right)\hbar\omega_0 + \hbar v_{\mathrm{F}}\langle\Psi_{\uparrow,N_0}|\sigma\cdot\mathbf{k}|\Phi(k)\rangle \\ &\quad = \varepsilon\,\mathcal{C}_{1,N_0}, \\ &\mathcal{C}_{2,N_0-1}\left(N_0 + \frac{\alpha^2}{4}\frac{N_0}{N_0-1}\right)\hbar\omega_0 \\ &\qquad + \hbar v_{\mathrm{F}}\langle\Psi_{\downarrow,N_0-1}|\sigma\cdot\mathbf{k}|\Phi(k)\rangle = \varepsilon\mathcal{C}_{2,N_0-1}, \\ &\mathcal{C}_{1,N_0+1}\left[(N_0+1) - \frac{\alpha^2}{4}\frac{N_0+2}{N_0+1}\right]\hbar\omega_0 \\ &\qquad + \hbar v_{\mathrm{F}}\langle\Psi_{\uparrow,N_0+1}|\sigma\cdot\mathbf{k}|\Phi(k)\rangle = \varepsilon\mathcal{C}_{1,N_0+1}, \\ &\mathcal{C}_{2,N_0}\left[(N_0+1) + \frac{\alpha^2}{4}\frac{N_0+1}{N_0}\right]\hbar\omega_0 \\ &\qquad + \hbar v_{\mathrm{F}}\langle\Psi_{\downarrow,N_0}|\sigma\cdot\mathbf{k}|\Phi(k)\rangle = \varepsilon\mathcal{C}_{2,N_0}. \end{aligned} \tag{15}$$

For chosen number N_0, each pair of these equations describes two energy subbands that are separated by $\backsim\alpha^2\hbar\omega_0/2$ at $k = 0$. Here, we include only the four nearest energy subbands, corresponding to the dressed states with different photon occupation numbers N and electron states with subband indices $\uparrow$ (lower energy) and $\downarrow$ (higher energy).

Taking into account the following relations for the Dirac Hamiltonian:

$$\begin{aligned} \sigma\cdot\mathbf{k}|\Psi_{\uparrow,N_0}\rangle &= \mu_{N_0}k_{+}|\downarrow, N_0\rangle - \nu_{N_0}k_{-}|\uparrow, N_0+1\rangle, \\ \sigma\cdot\mathbf{k}|\Psi_{\downarrow,N_0}\rangle &= -\mu_{N_0}k_{-}|\uparrow, N_0+1\rangle - \nu_{N_0}k_{+}|\downarrow, N_0\rangle, \end{aligned} \tag{16}$$

and with the simplifications described above, we can explicitly write out the Dirac Hamiltonian terms in equations (15) and (15). The presence of photon occupation numbers does not follow from the dressed states Hamiltonian and cannot be determined just from the ratio between the photon field energy $N\hbar\omega_0$ and the electron–photon interaction amplitude w. It should result from the model of the circularly polarized light source. If we consider electrons near the K point such that the kinetic energy $\hbar v_{\mathrm{F}}\,k \backsim \alpha^2\hbar\omega_0/2$, we can retain only three photon occupation numbers $N_0 - 1$, N_0 and $N_0 + 1$, which is consistent with the approximation described above. Consequently, we arrive at a system which consists of weakly coupled equations to determine the two nearest subbands, i.e.,

$$\left[\begin{array}{cc|cc} N_0\hbar\omega_0 - \Delta & -\mu^2\hbar v_{\mathrm{F}}k_{-} & \mu\nu\hbar v_{\mathrm{F}}k_{+} & 0 \\ \mu^2\hbar v_{\mathrm{F}}k_{+} & N_0\hbar\omega_0 + \Delta & 0 & -\nu\mu\hbar v_{\mathrm{F}}k_{+} \\ \hline -\nu\mu\hbar v_{\mathrm{F}}k_{-} & 0 & (N_0+1)\hbar\omega_0 - \Delta & -\mu^2\hbar v_{\mathrm{F}}k_{-} \\ 0 & \nu\mu\hbar v_{\mathrm{F}}k_{-} & \mu^2\hbar v_{\mathrm{F}}k_{+} & (N_0+1)\hbar\omega_0 + \Delta \end{array}\right] \times \begin{bmatrix} C_1 \\ C_2 \\ C_3 \\ C_4 \end{bmatrix} = \varepsilon \begin{bmatrix} C_1 \\ C_2 \\ C_3 \\ C_4 \end{bmatrix}, \tag{17}$$

where $\mu \equiv \mu_{N_0}$, $\nu \equiv \nu_{N_0}$, $\Delta \backsim \alpha^2\hbar\omega_0/4$, $C_1 \equiv C_{1,N_0}$, $C_2 \equiv C_{2,N_0-1}$, $C_3 \equiv C_{1,N_0+1}$ and $C_4 \equiv C_{2,N_0}$. This leads to the following energy dispersions with $\mu \approx 1$:

$$\begin{aligned} \varepsilon_{1,2}(k) &= (N_0 + \tfrac{1}{2})\hbar\omega_0 \\ &\quad - \tfrac{1}{2}\hbar\omega_0\sqrt{1 + \eta + \xi(1+\nu^2)k^2 \pm 2\sqrt{(\xi\nu^2k^2+1)(\xi k^2+\eta)}}, \end{aligned} \tag{18}$$

$$\begin{aligned} \varepsilon_{3,4}(k) &= (N_0 + \tfrac{1}{2})\hbar\omega_0 \\ &\quad + \tfrac{1}{2}\hbar\omega_0\sqrt{1 + \eta + \xi(1+\nu^2)k^2 \mp 2\sqrt{(\xi\nu^2k^2+1)(\xi k^2+\eta)}}, \end{aligned} \tag{19}$$

where $\xi = (2v_{\mathrm{F}}/\omega_0)^2$ and $\eta = (2\Delta/\hbar\omega_0)^2 \approx \alpha^4/4$.

Another approximation which we may used here is to consider only small wave vectors k so that we get two independent pairs of subbands separated by energy $\hbar\omega_0$. Let us estimate the order of magnitude for each off-diagonal element in the Hamiltonian (17). Using the relations in equations (12), we know that the expansion coefficients are $\mu \backsim 1$ and $\nu \backsim \alpha$, where $\alpha \ll 1$ is the ratio between the electron–photon interaction energy and the photon energy $\hbar\omega_0$. Note that the energy gap is $\Delta = \alpha^2\hbar\omega_0/4 \backsim \mathcal{O}(\alpha^2)$. Now let us consider small momenta k such that $\hbar v_{\mathrm{F}}k \backsim \alpha^2\hbar\omega_0$. As a result, we find that $\pm\mu^2\hbar v_{\mathrm{F}}k_{\pm} \backsim \alpha^2\hbar\omega_0 \backsim \mathcal{O}(\alpha^2)$ and $\pm\mu\nu\hbar v_{\mathrm{F}}k_{\pm} \backsim \alpha^3\hbar\omega_0 \backsim \mathcal{O}(\alpha^3) \to 0$. After all the $\mathcal{O}(\alpha^3)$ terms in equation (17) are neglected, we obtain

$$\left[\begin{array}{cc|cc} N_0\hbar\omega_0 - \Delta & -\mu^2\hbar v_{\mathrm{F}}k_{-} & 0 & 0 \\ \mu^2\hbar v_{\mathrm{F}}k_{+} & N_0\hbar\omega_0 + \Delta & 0 & 0 \\ \hline 0 & 0 & (N_0+1)\hbar\omega_0 - \Delta & -\mu^2\hbar v_{\mathrm{F}}k_{-} \\ 0 & 0 & \mu^2\hbar v_{\mathrm{F}}k_{+} & (N_0+1)\hbar\omega_0 + \Delta \end{array}\right] \times \begin{bmatrix} C_1 \\ C_2 \\ C_3 \\ C_4 \end{bmatrix} = \varepsilon \begin{bmatrix} C_1 \\ C_2 \\ C_3 \\ C_4 \end{bmatrix}. \tag{20}$$

This gives us two independent pairs of energy subbands and the corresponding two independent parts of the wavefunction. Each independent part is a two-component spinor wavefunction, where each component consists of two independent terms.

The corresponding eigenvalue equation for the case of two independent pairs of subbands yields, as expected,

$$\{\hbar^2 v_F^2 k^2 + \Delta^2 - (\varepsilon - N_0\hbar\omega_0)^2\}\{\hbar^2 v_F^2 k^2 + \Delta^2 - [\varepsilon - (N_0+1)\hbar\omega_0]^2\} = 0. \quad (21)$$

If we consider the transmission of such states through a potential barrier whose height is equal to $\hbar\omega_0$, one of the terms in region '1' will exactly match the other in region '2' (the potential region) so that a part of the wavefunction will be completely transmitted. This will lead to a substantial increase in the total transmission. On the other hand, if we consider a larger number of such subband pairs, this effect will not be significant since this complete transmission occurs only for one of the wavefunction terms. This is reminiscent of the Klein paradox since it does not depend on the barrier width as long as the barrier height is exactly equal to $\hbar\omega_0$. The revelation of such an anomalous increase for the dressed state tunneling is an important discovery of the present paper.

The simplest possible approximation is to keep only two terms with the coefficients $[\mathcal{C}_1(k), \mathcal{C}_2(k)]$ leading to the two nearest energy subbands separated by a gap $2\Delta \backsimeq \alpha^2\hbar\omega_0/2$ at $k = 0$ due to electron–photon interaction. The block-diagonal approximation introduced in equation (20) is valid only for a single value N_0 of photon number as well as small values of k. In this situation, the other subband pairs become far away from the considered one and, therefore, their influence can be neglected. We will use this approximation in the rest of our paper.

Equation (20) results in a simplified algebraic system determining the pair of coefficients $\mathcal{C}_1(k)$ and $\mathcal{C}_2(k)$, i.e.,

$$\begin{aligned}(N_0\hbar\omega_0 - \Delta)\,\mathcal{C}_1 + \hbar v_F(k_x + \mathrm{i}k_y)\mathcal{C}_2 &= \varepsilon\,\mathcal{C}_1,\\ (N_0\hbar\omega_0 + \Delta)\,\mathcal{C}_2 + \hbar v_F\,(k_x - \mathrm{i}k_y)\,\mathcal{C}_1 &= \varepsilon\,\mathcal{C}_2.\end{aligned} \quad (22)$$

The non-trivial solution of these equations gives the energy dispersion which was previously obtained in [9] as

$$\varepsilon(k) = N_0\hbar\omega_0 \pm \sqrt{\Delta^2 + \hbar^2 v_F^2 k^2} \equiv N_0\hbar\omega_0 + \beta\sqrt{\Delta^2 + \hbar^2 v_F^2 k^2}. \quad (23)$$

If the electron–photon interaction is removed, then $\alpha \equiv w/2 \to 0$, and the energy dispersion relations (23) demonstrate a non-interacting system consisting of a Dirac electron $\varepsilon_\beta(k) = \beta\hbar v_F|k|$ and photons $N_0\hbar\omega_0$. All the other energy subbands are separated at least by $\hbar\omega_0 \gg w$ and can be neglected, which justifies the above two-subband approximation. In this notation, $\beta = \pm 1$ is the dressed conduction/valence band index corresponding to bare electron/hole bands for infinite graphene when $\Delta \to 0$.

The system (22) is formally similar to the eigenvalue equations for the case of the effective mass Dirac Hamiltonian

$$\mathcal{H} = \hbar v_F\,\sigma\cdot\mathbf{k} + \mathcal{V}(x)\begin{bmatrix}1 & 0\\ 0 & 1\end{bmatrix} + \Delta\,\sigma_3, \quad (24)$$

where σ_3 is a Pauli matrix and $\mathcal{V}(x)$ is a one-dimensional potential. The electron dispersion and transmission properties for both a single as well as multiple square potential barriers have been studied [7, 11] for monolayer and bilayer graphene [12]. It was also shown that a one-dimensional periodic array of potential barriers leads to multiple Dirac points [13]. Several papers have introduced an effective mass term into the Dirac Hamiltonian for infinite graphene which may be justified based on different physical reasons [14]. For example, it has been shown [15] that an energy bandgap in graphene can be created by a boron nitride substrate, resulting in a finite electron effective mass. However, we emphasize that the analogy between the Hamiltonian (24) and that for irradiated graphene is not complete since that would correspond to $\Delta < 0$. Although this difference does not result in any modification of the energy dispersion term containing Δ^2, it certainly modifies the corresponding wavefunction. The occurrence of a tunable energy gap in graphene coupled to a laser source is discussed in [16].

It was demonstrated in [17, 18] that strained superlattices can be used to open an appreciable energy gap in the graphene energy spectrum and modify the spin–orbit interaction considerably. However the advantage of using a circularly polarized light is that the energy gap is tunable by varying the frequency and intensity of the applied optical field. In addition, we know that an energy gap can also be created by using the surface curvature [6]. However, for the case of curved or strained graphene, the longitudinal momentum is no longer a good quantum number and the translational symmetry is lost. As a result, the formalism presented in this paper for finding the transmission amplitude can no longer be applied to this case.

Instead, we consider another case in which the energy gap is created by a substrate and a circularly polarized light at the same time. In this case, we obtain the following Hamiltonian [19]:

$$\mathcal{H} = \hbar\omega_0\,\hat{a}^\dagger\hat{a} + \hbar v_F\,\sigma\cdot\mathbf{k} + \frac{\hbar\omega_0}{2}\,\sigma_3 - \alpha\hbar\omega_0(\sigma_+\hat{a} + \sigma_-\hat{a}^\dagger) = \hbar\omega_0\,\hat{a}^\dagger\hat{a} + H_{\mathrm{Dirac}} + \frac{\hbar\omega_0}{2}\,\sigma_3 + H_{\mathrm{J-C}}, \quad (25)$$

which gives rise to the energy dispersion

$$\varepsilon(k) = \sqrt{(\hbar v_F k)^2 + \Delta_{\mathrm{sub}}^2 + \Delta^2}. \quad (26)$$

Here, Δ_{sub} is the substrate-induced energy gap and Δ is the energy gap induced by the electron–photon interaction. The total energy gap is then given by $\Delta_{\mathrm{total}} = \sqrt{\Delta_{\mathrm{sub}}^2 + \Delta^2}$, where we only consider the case with two nearest energy subbands.

The interaction between the Dirac electrons in graphene and a circularly polarized light has been considered in the classical limit in [20]. In this limit, a gap in the Dirac cone opens up due to nonlinear effects. The dressed-state wavefunction has the form

$$\Phi_{\mathrm{dr}}(k) = \begin{bmatrix}\mathcal{C}_1(k)\\ \beta\mathcal{C}_2(k)\,\mathrm{e}^{\mathrm{i}\phi}\end{bmatrix}, \quad (27)$$

with $\mathcal{C}_1(k) \neq \mathcal{C}_2(k)$ given by

$$\mathcal{C}_1^{\pm}(k) = \frac{1}{\sqrt{2(1+\gamma^2) \mp 2\gamma\sqrt{1+\gamma^2}}}, \quad (28)$$

$$\mathcal{C}_2^{\pm}(k) = \pm\frac{\sqrt{1+\gamma^2}\mp\gamma}{\sqrt{2(1+\gamma^2)\mp 2\gamma\sqrt{1+\gamma^2}}}, \tag{29}$$

corresponding to the energy subbands $\varepsilon(k) = N_0\hbar\omega_0 \pm \sqrt{\Delta^2+\hbar^2 v_{\mathrm{F}}^2 k^2}$. In this notation, $\gamma = \Delta/(\hbar v_{\mathrm{F}} k)$ and ϕ is the angle which $\mathbf{k}$ makes with the longitudinal x axis. Without an optical field, i.e. $\Delta = 0$, we obtain $\mathcal{C}_1^{\pm} = \mathcal{C}_2^{\pm} = 1/\sqrt{2}$. In the limit ($\Delta \ll k$), the coefficients exhibit peculiar symmetry with

$$\begin{aligned}\mathcal{C}_{1,2}^{+}(k) &\backsimeq \frac{1}{\sqrt{2}} \pm \frac{\gamma}{2\sqrt{2}} - \frac{\gamma^2}{8\sqrt{2}} \mp \frac{3\gamma^3}{16\sqrt{2}},\\ \mathcal{C}_{1,2}^{-}(k) &\backsimeq \pm\frac{1}{\sqrt{2}} - \frac{\gamma}{2\sqrt{2}} \mp \frac{\gamma^2}{8\sqrt{2}} + \frac{3\gamma^3}{16\sqrt{2}}.\end{aligned} \tag{30}$$

We note that this expansion is not valid too close to the Dirac point and should not be used for an arbitrary wave vector to calculate, for example, the polarization function. Additionally, one may verify that $\mathcal{C}_1(k) \neq \mathcal{C}_2(k)$ for any chosen Δ in the range of validity. Consequently, the chiral symmetry is broken for electron dressed states

$$\hat{h}\Psi_{\mathrm{dr}}(k) = \frac{1}{2}\frac{\sigma\cdot\mathbf{p}}{p}\begin{bmatrix}\mathcal{C}_1(k)\\ \beta\mathcal{C}_2(k)\,\mathrm{e}^{\mathrm{i}\phi}\end{bmatrix} = \frac{1}{2}\begin{bmatrix}\beta\mathcal{C}_2(k)\\ \mathcal{C}_1(k)\,\mathrm{e}^{\mathrm{i}\phi}\end{bmatrix}. \tag{31}$$

Clearly, it follows from (31) that the non-chirality of the dressed electron states becomes significant if the electron–photon interaction (the leading γ term) is increased. This affects the electron tunneling and transport properties. We now turn to an investigation of the transmission of electron states through a potential barrier when graphene is irradiated with a circularly polarized light.

For simplicity, we consider a square potential barrier of height V_0 given by $\mathcal{V}(x) = V_0[\theta(x) - \theta(x - W_0)]$, where W_0 is the barrier width and $\theta(x)$ is the Heaviside step function. Since the wave number k_x is the same in regions 1 ($x < 0$) and 3 ($x > W_0$) and the current component is $j_x = \Phi^{\dagger}\sigma_x\Phi$, we only need the wavefunction continuity at the potential boundaries for the system considered. From this continuity condition, the transmission probability T can be determined from $T = |t|^2$, where t is the transmission coefficient or the amplitude of the wave propagating forward in region 3. Here, we only show an analytical expression for the transmission coefficient of the dressed states in the limit of $\varepsilon \ll V_0$ corresponding to $k_{x1} \ll k_{x2}$:

$$\begin{aligned}T = {} & \frac{\cos^2\phi}{\cos^2(k_{x2}W_0)\cos^2\phi + \sin^2(k_{x2}W_0)}\\ & - \frac{3\cos^2(k_{x2}W_0)\cos^2\phi\sin^2(k_{x2}W_0)}{\hbar^2 v_{\mathrm{F}}^2 k_{x1}^2[\sin^2(k_{x2}W_0) + \cos^2(k_{x2}W_0)\cos^2\phi]}\Delta^2.\end{aligned} \tag{32}$$

Here, $\theta = \tan^{-1}(k_y/k_{x2}) \to 0$, $\phi = \tan^{-1}(k_y/k_{x1})$, the second term includes the effect of electron–photon interaction ($\propto\Delta^2$) to the leading order. In addition, we only show those terms of the lowest order in ε/V_0. There is another relevant study [21], investigating the tunneling of Dirac electrons with a finite effective mass, a parabolic dispersion in the presence of an energy gap, and a certain chirality, through a potential region. In that study, a particle tunneling through a square potential barrier differs from both the Dirac electrons and the dressed states of electrons under a circularly polarized light illumination.

For nearly head-on collision with $k_y \ll k_{x1} \ll k_{x2}$ for high potential as well as for infinite graphene ($\Delta \to 0$), the transmission coefficient has the following simplified form:

$$T = 1 - \sin^2(k_{x2}W_0)(\theta^2 - 2\beta\theta\phi + \phi^2), \tag{33}$$

where we assume $V_0 \gg \varepsilon, \theta \ll \phi \ll 1$ and $\beta = \pm 1$.

3. Numerical results and discussion

In our numerical calculations, energies will be measured in units of $(3k_{\mathrm{F}}at/2)$ with the carbon–carbon distance $a \approx 1.42$ Å and the hopping parameter $t = 2.7\sqrt{3}/2$ eV. We measure the wave vector in units of the Fermi wave number k_{F} and write its components as $k_x = \cos\phi$ and $k_y = \sin\phi$ in terms of the angle of incidence ϕ.

In figure 1, we present the transmission for dressed electron states with arbitrary energy and angle of incidence. We clearly see that dressing ruins the Klein paradox in (a) for head-on collision with $\phi = 0$. The resonant peaks are shifted for the other incoming angles in (b) and the effect is stronger for small incident angles. In (c) and (d), the transmission probability plots are given in terms of the longitudinal momentum k_{x1} in front of the barrier and k_{x2} in the barrier region. We find that the intensities and locations of the transmission peaks in (d) are distorted compared to those for infinite graphene in (c). The diagonal $k_{x1} = k_{x2}$ corresponds to the absence of a potential barrier and should yield a complete transmission for $\Delta = 0$. However, the condition $(\sqrt{(\varepsilon - V_0)^2 - \Delta^2} > \hbar v_{\mathrm{F}} k_y)$ for dressed states must be satisfied, which makes the diagonal incomplete (missing diagonal for small k_{x1} and k_{x2}) due to the occurrence of an induced gap.

Figure 2 displays the effect due to the electron–photon interaction on the electron transmission in terms of incoming particle energy ε and angle of incidence ϕ. From the figure, we see the Klein paradox as well as resonant tunneling peaks in the transmission probability for regular infinite graphene with $\Delta = 0$ in (a). The dark 'pockets' on both sides of $\varepsilon = V_0$ in (a) demonstrate zero transmission for the case $|\varepsilon - V_0| \ll \varepsilon$, which results in imaginary longitudinal momenta k_{x2} for most incident angles and produces a completely attenuating wavefunction. When a small gap is opened in (b) for the dressed states of electrons in graphene under illumination by a circularly polarized light, we observe a set of complete transmission branches, where a strong dependence on ϕ for the lower branches is seen. However, this ϕ dependence is greatly suppressed when the dressed-state gap is increased in (c), leaving us a set of equally distant branches due to photo-assisted electron tunneling.

As mentioned above, by including more than the two nearest subbands, as shown in figure 3(a), the electron dispersion, wavefunction and transmission amplitude will be modified. According to the approximation adopted by Kibis [9], the two subband pairs may be considered as independent. Under the condition of equal transverse

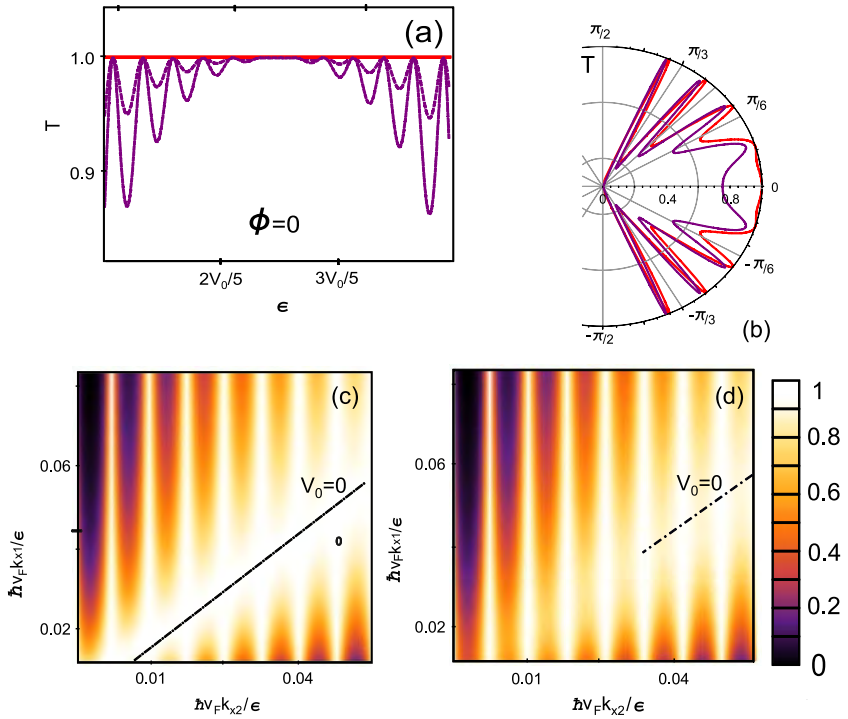

Figure 1. Transmission probability T of electrons as functions of incoming energy ε, incident angle ϕ, and longitudinal wave numbers $\hbar v_F\, k_{x1}$ and $\hbar v_F\, k_x$. In (a), the transmission probability (purple dashed curve) is plotted as a function of the incident particle energy for head-on collision ($\phi = 0$). The red solid line is the transmission probability $T = 1$ (Klein paradox) for infinite graphene when the energy gap $\Delta = 0$. In (b), we show the angular distributions of T for infinite graphene (solid red curve) and the dressed states (purple dashed curve) with $\varepsilon = V_0/6$. In (c) and (d), the transmission probability is plotted as a function of the longitudinal momenta in regions '1' and '2' (before the potential barrier and in the barrier region, respectively) for infinite graphene (c) and irradiated graphene (d). The diagonal $k_{x1} = k_{x2}$ corresponds to the absence of a potential barrier ($V_0 = 0$) and displays a perfect transmission with $T = 1$ as long as both longitudinal momenta are real determined by both the barrier height V_0 and the energy gap Δ.

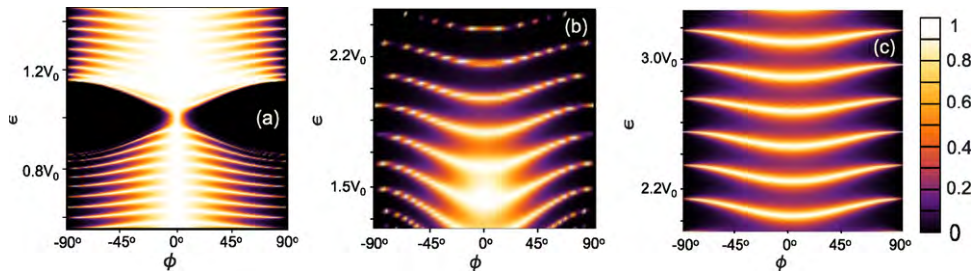

Figure 2. Transmission probability T as functions of both the incoming electron energy ε and the angle of incidence ϕ. Plot (a) is for infinite graphene ($\Delta = 0$) with the obvious Klein paradox for $\phi = 0$. Plots (b) and (c) show the transmission T for electron dressed states, in the two nearest subbands approximation, with gap energies $\Delta = V_0/15$ (b) and $\Delta = V_0/5$ (c).

momentum k_y for both terms of the particle wavefunction, the first term of the wavefunction in region '2' with a potential barrier is similar to the second term in the regions without potential. Therefore, the states exactly match across the potential boundary, which should definitely increase the total transmission amplitude. The other possibility is that incoming angle and momentum of the second term are totally independent of the first one and lead to resonant transmission regardless of the transmission amplitude of the first term. Based on our derived results, we find that the transmission should increase even for non-split energy subband pairs and corresponding wavefunctions. Since the existence of certain photon occupation numbers N is determined by the laser source, we can consider that only one pair of the dressed state subbands is occupied while the other subband pairs are unpopulated. As illustrated in figure 3(b), in the potential region '2', a particle may populate another subband corresponding to a different number of photons instead of changing its longitudinal momentum for barrier heights exactly equal to a multiple of $\hbar\omega_0$. The opposite transition will occur at the boundary between regions '2' and '3'. This will result in unimpeded tunneling $T = 1$ independent of the barrier width, as seen from figure 3(c), which is expected to be a major contribution to the current.

We now investigate the effect of disorder on the transmission probability through a potential barrier in graphene. This can appear as short-range disorder, inter-valley scattering and trigonal distortion. In single layer graphene,

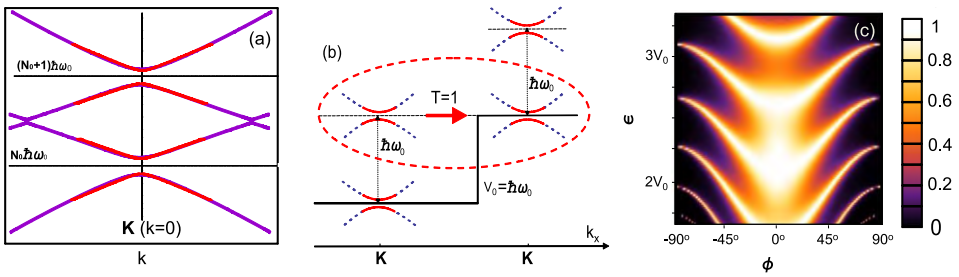

Figure 3. Energy dispersion and transmission probability for the case of two independent pairs of energy subbands. Panel (a) shows the energy dispersion by taking into account the coupling between the states corresponding to two different photon occupation numbers in the linear approximation. In (b), we present a schematic diagram showing how the transmission probability may be increased due to the presence of the other energy subbands. Panel (c) gives the transmission versus the incoming particle energy and the angle of incidence for the case of two independent pairs of energy subbands.

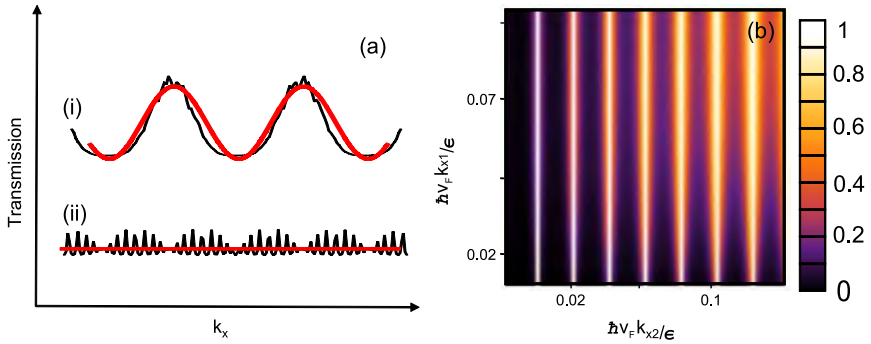

Figure 4. Effect of disorder on the transmission probability using the Lorentzian distribution model. In panel (a) we plot in (i) the transmission probability as a function of k_{x1} for dressed electrons (black curve) compared to infinite graphene (red curve) for head-on collision. The plot in (ii) shows a two-peak model distribution under the influence of disorder. In panel (b) we show the transmission probability for electron dressed states with $\Delta = V_0/3$ in the presence of disorder.

disorder also induces a metal–insulator transition by creating a dynamical gap [22]. Consequently, this effect can modify the gap created by the electron–photon interaction. In bilayer graphene, disorder directly leads to energy dispersion with a gap as well as modifying the energy dispersion close to the band edges. Additionally, disorder may also lead to localized states inside a gap in bilayer graphene [23, 24].

In this paper, we introduce disorder phenomenologically through the non-conservation of the transverse electron momentum k_y. As mentioned above, k_y is conserved for both Dirac electrons in infinite graphene and states dressed by photons. Introducing the quantity Γ as a measure for the disorder [25, 26], we model its stochastic distribution as a Lorentzian, yielding

$$t_{\rm dis}(k_x,\, k_y) = \frac{\Gamma}{\pi}\int_{-\infty}^{\infty} {\rm d}q_y\, \frac{t_0(k_x,\, q_y)}{(k_y - q_y)^2 + \Gamma^2}, \qquad (34)$$

where $t_0(k_x,\, q_y)$ denotes the transmission coefficient in the absence of any imperfections. As long as the disorder is weak with $\Gamma \ll 1$, different distributions, which give the δ-function in the limit of $\Gamma \to 0$, will result in almost equal transmission coefficients. For nearly head-on collision, $k_y \ll k_{x2}$, the transmission coefficient may be obtained analytically using a Gaussian distribution. The imperfect boundary of the potential region can also be the result of some stochasticity of k_{x2} to make the effect stronger. We neglect this effect since our goal is to investigate the role played by disorder using a simple approximation.

Our numerical results showing the effect due to disorder are presented in figure 4. First we test our numerical results in (a) by applying the Lorentzian transformation in (34) to the complete transmission with $T = 1$, corresponding to the Klein paradox with head-on collision for infinite graphene. Analytical integration clearly results in a transmission amplitude equal to unity. The transformed distribution demonstrates the precision of our numerical procedure. By comparing figure 4(b) with figure 1(d), we see a complete suppression of the perfect transmission with $T = 1$ along the diagonal $k_{x1} = k_{x2}$ by disorder along the boundary as well as a reduced range of k_{x2} for photon-assisted perfect transmission.

4. Concluding remarks

According to recently published results [9], the interaction between Dirac particles in graphene and circularly polarized light leads to the formation of quantum electron dressed states. These states are appreciably different from conventional Dirac electrons in ordinary infinite graphene. From [9], a laser power of 100 mW leads to a gap of the order of $\Delta \backsimeq 100$ meV, which is required to make the effect significant for infrared light frequencies and room temperature. This enables possible experimental demonstrations of the described effects. We have shown that the electron–photon interaction gives rise to states of broken chiral symmetry. The non-symmetrical properties of the states become more significant when the electron–photon interaction is increased. In addition, there are no dressed states

with chirality symmetry. In general, incoming electrons or holes passing unimpeded through a square potential barrier require chiral symmetry. Under illumination from a circularly polarized light, we can control the degree of partially broken chiral symmetry in dressed states or the degree of partially perfect transmission through a potential barrier in a graphene layer.

In the simplest approximation when only the two nearest subbands are included, the model is formally similar to the so-called σ_3 Hamiltonian used to describe the particles in single layer graphene with parabolic energy dispersion, giving non-zero electron effective mass. We have discussed the similarities as well as the differences affecting the wavefunctions but not the energy dispersion. We have also studied in detail both numerically and analytically how the transmission probability depends on the angle of incidence or on the incoming energy for the case of head-on collision.

By including more of the next-nearest subbands, the tunneling amplitude is modified in a significant way. In the approximation when two independent pairs of subbands are included, we obtain an enhanced transmission probability when the barrier height is close to $\hbar\omega_0$. This is due to the fact that one of the terms in the corresponding wavefunction could be perfectly transmitted. We have analytically obtained the energy dispersions for this case. By including more than two independent pairs, this effect will decrease since perfect transmission will occur only for the two wavefunction terms. The effect is not sensitive to the barrier width, and, therefore, can be considered as reminiscent of the Klein paradox.

We have introduced disorder phenomenologically in this paper through non-conservation of the transverse electron momentum component, which is shown to suppress the perfect transmission along the diagonal $k_{x1} = k_{x2}$. From a physical point of view, this disorder model could be interpreted as arising from the surface roughness of the potential barrier. The same type of statistical distribution can be applied to fluctuations in the barrier width which will result in modification of the intensity and location of the transmission peaks. Consequently, the transmission maxima observed experimentally will not exactly match those theoretically predicted for clean samples.

Acknowledgments

This research was supported by contract # FA 9453-11-01-0263 of the AFRL. DH would like to thank the Air Force Office of Scientific Research (AFOSR) for its support.

References

[1] Geim A K, Morozov S V, Jiang D, Katsnelson M I, Grigorieva I V, Dubonos S V, Firsov A A and Novoselov K S 2005 Two-dimensional gas of massless dirac fermions in graphene *Nature* **438** 197–200

[2] Geim A K 2009 Graphene: status and prospects *Science* **324** 1530–4

[3] Castro Neto A H, Guinea F, Peres N M R, Novoselov K S and Geim A K 2009 The electronic properties of graphene *Rev. Mod. Phys.* **81** 109–62

[4] Katsnelson M I, Novoselov K S and Geim A K 2006 Chiral tunnelling and the klein paradox in graphene *Nature Phys.* **2** 620–5

[5] Chevianov Vadim V and Fal'ko V I 2006 Selective transmission of Dirac electrons and ballistic magnetoresistance of n–p junctions in graphene *Phys. Rev.* B **74** 041403

[6] Atanasov V and Saxena A 2010 Tuning the electronic properties of corrugated graphene: confinement, curvature, and band-gap opening *Phys. Rev.* B **81** 205409

[7] Barbier M, Peeters F M, Vasilopoulos P and Milton Pereira J 2008 Dirac and Klein–Gordon particles in one-dimensional periodic potentials *Phys. Rev.* B **77** 115446

[8] McCann E and Fal'ko V I 2006 Landau-level degeneracy and quantum hall effect in a graphite bilayer *Phys. Rev. Lett.* **96** 086805

[9] Kibis O V 2010 Metal–insulator transition in graphene induced by circularly polarized photons *Phys. Rev.* B **81** 165433

[10] Kibis O V 2011 Dissipationless electron transport in nanostructures dressed by photons arXiv:1103.0950

[11] Barbier M, Vasilopoulos P and Peeters F M 2009 Dirac electrons in a Kronig–Penney potential: dispersion relation and transmission periodic in the strength of the barriers *Phys. Rev.* B **80** 205415

[12] Barbier M, Vasilopoulos P, Peeters F M and Milton Pereira J 2009 Bilayer graphene with single and multiple electrostatic barriers: band structure and transmission *Phys. Rev.* B **79** 155402

[13] Barbier M, Vasilopoulos P and Peeters F M 2010 Extra dirac points in the energy spectrum for superlattices on single-layer graphene *Phys. Rev.* B **81** 075438

[14] Low T, Guinea F and Katsnelson M I 2011 Gaps tunable by electrostatic gates in strained graphene *Phys. Rev.* B **83** 195436

[15] Giovannetti G, Khomyakov P A, Brocks G, Kelly P J and van den Brink J 2007 Substrate-induced band gap in graphene on hexagonal boron nitride: *ab initio* density functional calculations *Phys. Rev.* B **76** 073103

[16] Calvo H L, Pastawski H M, Roche S and Foa Torres L E F 2011 Tuning laser-induced band gaps in graphene *Appl. Phys. Lett.* **98** 232103

[17] Guinea F, Katsnelson M I and Geim A K 2010 Energy gaps, topological insulator state and zero-field quantum Hall effect in graphene by strain engineering *Nature Phys.* **6** 30–3

[18] Huertas-Hernando D, Guinea F and Brataas A 2006 Spin–orbit coupling in curved graphene, fullerenes, nanotubes, and nanotube caps *Phys. Rev.* B **74** 155426

[19] Gerry C and Knight P 2005 *Introductory Quantum Optics* (Cambridge: Cambridge University Press)

[20] Oka T and Aoki H 2009 Photovoltaic Hall effect in graphene *Phys. Rev.* B **79** 081406

[21] Viana Gomes J and Peres N M R 2008 Tunneling of dirac electrons through spatial regions of finite mass *J. Phys.: Condens. Matter* **20** 325221

[22] Mildenberger A, Evers F, Mirlin A D and Chalker J T 2007 Density of quasiparticle states for a two-dimensional disordered system: metallic, insulating, and critical behavior in the class-d thermal quantum Hall effect *Phys. Rev.* B **75** 245321

[23] Mkhitaryan V V and Raikh M E 2008 Disorder-induced tail states in gapped bilayer graphene *Phys. Rev.* B **78** 195409

[24] Ferreira A, Viana-Gomes J, Nilsson J, Mucciolo E R, Peres N M R and Castro Neto A H 2011 Unified description of the dc conductivity of monolayer and bilayer graphene at finite densities based on resonant scatterers *Phys. Rev.* B **83** 165402

[25] Abranyos Y, Gumbs G and Fekete P 2010 Spin-dependent scattering by a potential barrier on a nanotube *J. Phys.: Condens. Matter* **22** 505304

[26] Wang D W and Das Sarma S 2001 Elementary electronic excitations in one-dimensional continuum and lattice systems *Phys. Rev.* B **65** 035103